10

Development of technology for creating photonic ICs with ring microresonators based on $Si/SiO_2/Si_3N_4$

© A.I. Abanin[1,2,3], R.M. Ryazanov[1], A.D. Golikov[4,5], V.V. Kovalyuk[4,6], I.O. Venediktov[4,6], P.P. An[4,5], D.A. Shimlovskaya[7], E.P. Kitsyuk[1], S.S. Kosolobov[7], P.I. Lazarenko[3], G.N. Goltsman[6,8], V.V. Svetukhin [1]

[1] Scientific-Manufacturing Complex „Technological Centre“, Moscow, Zelenograd, Russia
[2] Ulyanovsk State University, Ulyanovsk, Russia
[3] National Research University of Electronic Technology, Zelenograd, Moscow, Russia
[4] National University of Science and Technology MISiS, Moscow, Russia
[5] Moscow Pedagogical State University, Moscow, Russia
[6] National Research University Higher School of Economics, Moscow, Russia
[7] Skolkovo Institute of Science and Technology, Moscow, Russia
[8] Russian Quantum Center, Moscow, Russia

e-mail: aai-2000@mail.ru

Received June 06, 2025
Revised September 09, 2025
Accepted September 10, 2025

The development of modern information processing systems is limited by the speed of electronic circuits. The implementation of high-speed information processing of the next generation becomes an extremely difficult task while using a traditional electronic component database. One of the possible solutions to this problem is developing systems based on photonic integrated circuits. In this paper, we present the results of manufacturing high-Q ring resonators based on silicon nitride. Optical devices were manufactured on $Si/SiO_2/Si_3N_4$ substrates, using fabrication equipment of the SMC "Technological Centre". In this work, we studied the dependence of optical properties of structures on different deposition methods for silicon nitride, as well as the use of high-temperature annealing. Samples of ring resonators with $> 10^5$ and ring radius of $\approx 64\,\mu$m microns are demonstrated.

Keywords: Silicon nitride, ring resonator, LPCVD, Q-factor.

DOI: 10.61011/EOS.2025.09.62308.8228-25

Introduction

Photonic integrated circuits (PICs) are essential components of modern photonic and radio-photonic devices. The use of PICs eliminates the need for discrete optical components, providing miniaturization, increased reliability, and reduced cost of developed systems [1–4], which, together with the possibility of manufacturing them using existing microelectronics production facilities, has driven active development in this field in recent decades.

The material of the integrated platform from which PICs are made significantly influences the functionality and size-weight characteristics of the devices. Currently, the most widely used platforms include InP [5,6], Si_3N_4 [7–14] and silicon on insulator (SOI) [15–20]. However, the choice of material for PIC manufacture is usually a compromise. Although silicon nitride has a significantly lower thermo-optic coefficient and a lower refractive index compared to the SOI platform — which substantially limits high-speed applications and complicates hybrid coupling — waveguides based on it exhibit lower optical propagation losses and a higher nonlinear threshold, which, for example, allows the use of silicon nitride PICs to create tunable and narrow-band lasers.

Despite numerous scientific works on this topic, there remains the problem of the lack of a refined manufacturing technology for forming $Si/SiO_2/Si_3N_4$ structures suitable for PIC production. The problem lies in the fact that due to the large length of even individual PIC elements (tens and hundreds of wavelengths), investigating material losses by conventional ellipsometry or refractometry methods — where radiation interacts with the film at a small angle — does not allow optimization of film formation processes. Therefore, alongside material studies, this work involved research on fabricated optical structures and determination of technological regimes' effects on their parameters.

This work presents results on refining technological processes for forming $Si/SiO_2/Si_3N_4$ structures and subsequently creating integrated microcavities based on them for measuring optical losses in silicon nitride.

Refinement of Formation Regimes for SiO_2 and Si_3N_4Layers

The processes for forming SiO_2 and Si_3N_4 layers were developed at the production facility of Scientific-Industrial Complex „Technology center“ on silicon wafers of KEF 4,5 (100) grade, 100 mm diameter. Before technological operations, wafers underwent cleaning in CARO (H_2SO_5) and PAR (peroxide-ammonia solution).

The SiO_2 layer was formed by thermal oxidation of silicon wafers in water vapor under pressure using the „Termokom-M“ setup. Studies established that thermal oxidation of Si at 1000 °C and 10 at pressure yields uniform, high-purity SiO_2 layers with minimal surface roughness and a refractive index suitable for PICs.

After oxidation, wafers were examined with an optical profilometer „FRT MicroProf 100“ to determine average wafer stress along eight axes. The deformation study showed no significant flatness distortions after forming thick SiO_2 layers. For example, flatness deviations for 100 mm wafers before and after forming a SiO_2 thick 2.7 μm layer were 5 and μm respectively. This outcome was achieved by using double-sided polished silicon wafers, allowing symmetrical oxide formation on both the front and back sides.

The next step was forming a silicon nitride layer of a specified thickness by low-pressure chemical vapor deposition (LPCVD) on the HCVD-55 setup. The process used a gas mixture of dichlorosilane (SiH_2Cl_2) and ammonia (NH_3). Different deposition temperature regimes (350 and 750 °C) were tested to form amorphous Si_3N_4 layers approximately 450 nm thick. The effect of annealing was also studied: some wafers underwent annealing in a thermodiffusion furnace in Si_3N_4 in N_2 at 1200 °C to remove hydrogen.

The thickness and optical parameters of the formed $Si/SiO_2/Si_3N_4$, structures were studied using ellipsometry on a „SENDURO“ setup by „SENTECH“. This method provided refractive index values for Si_3N_4 and SiO_2 layers. Ellipsometry results confirmed good reproducibility of thicknesses and refractive indices of the layers. Calculated refractive indices and thicknesses were 1.47 and 2.7 $\pm$ 0.3 μm for SiO_2 and 2.05 and 450 $\pm$ 10 nm. for Si_3N_4.

Manufacture of Ring Microcavities

The study developed a design consisting of a ring resonator, waveguides, and optical input-output elements. Patterns for element topology formation were created in Python, enabling single elements or matrices of devices with different parameters. Figure 1 shows the designed pattern image for an electron-beam lithographer.

Identical series of ring microresonators with a ring radius of 64 μm and different gap widths (w_g) between waveguide and ring in the coupling region were fabricated on all crystal samples. The gap size ranged from 0.4 to 1 μm. Diffraction gratings (FGC in Fig. 1) served as input elements. Structures were fabricated by electron-beam lithography followed by plasma-chemical etching of silicon nitride in Ar and CHF_3 gas mixture using the „CORIAL-200R“ setup (manufacturer: „Plasma-Therm“).

Waveguide profiles were comb-shaped, etched to half the silicon nitride layer height. Geometric parameters were controlled by optical, scanning electron, and atomic force microscopy. or comparative analysis, waveguide elements with ring microcavities were made both on substrates from SIC „Ttechnology center“ and on commercially produced $Si/SiO_2/Si_3N_4$ substrates with similar layer thicknesses.

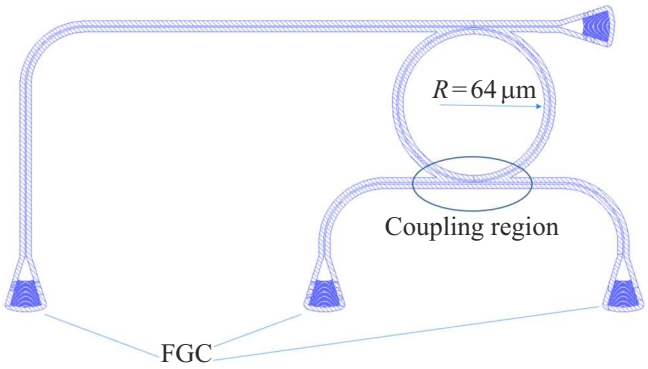

Figure 1. Developed electron-beam lithography template for fabricating integrated optical devices. R — ring radius, FGC — focusing grating coupler, Coupling region — optical coupling area.

Methodology for Studying Spectral Characteristics of Resonant Cavity Optical Structures

The optical characteristics of ring resonators were calculated from their transmission spectra obtained in the wavelength range 1480 to 1640 nm using the experimental setup shown in Fig. 2, *a*. Light from a narrowband tunable laser source („TSL-710“, Santec) passed through a polarization controller („FPC030“, Thorlabs) and optical fiber array („SQS Vláknova, 12ch“) to the input of the manufactured ring resonant cavity positioned on a movable stage. Movement between elements of the variable matrix of ring microcavities was controlled by a piezo-positioner („New Focus 8303“), driven by a controller and visually monitored by a video camera („CMOS CS135MUN“, Thorlabs). The output power of the ring resonator was measured by a photodetector („G-9801“, Hamamatsu) allowing spectral characterization of samples in combination with laser wavelength tuning.

Obtained spectral dependencies allow determination of the free spectral range (FSR) as the distance between adjacent resonances (Fig. 3, *a*).

Further parameter determination of fabricated elements was performed by approximating the obtained spectral dependencies. Resonance peaks were approximated by the Lorentz function (Fig. 4, *b*), which was used to estimate the loaded quality factor of the ring resonant cavity (Q_{load}) calculated as follows:

$$Q_{\text{load}} = \frac{\lambda_0}{FWHM}, \tag{1}$$

where λ_0 is the resonance wavelength and $FWHM$ FWHM (English: Full width at half maximum) is the full width at half maximum height.

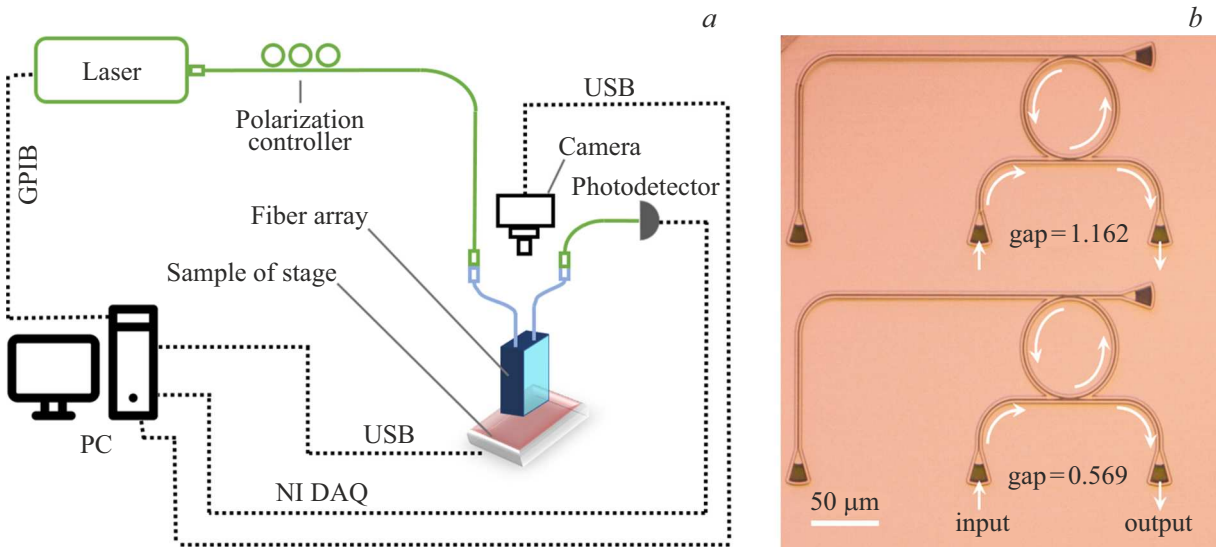

Figure 2. Measurement setup scheme (*a*) and optical microscope image of formed elements (*b*).

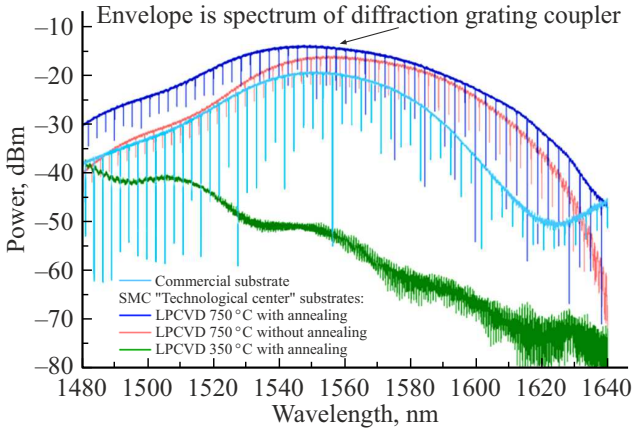

Figure 3. Comparison of spectral characteristics of ring resonant cavities made on different substrates.

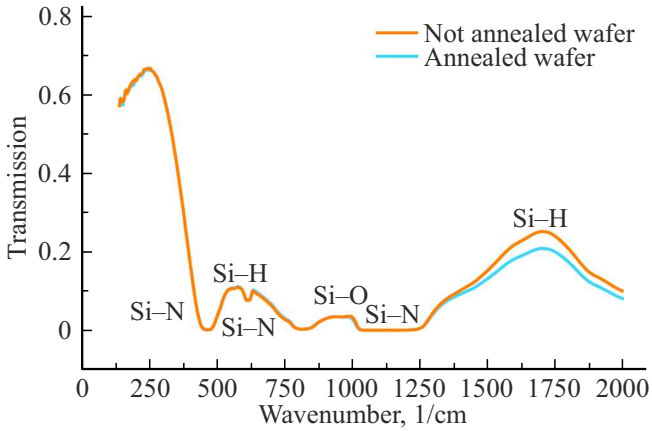

Figure 4. FTIR spectra of structures before and after annealing.

The loaded quality factor Q_{load} in turn, allows determination of the intrinsic quality factor of the ring resonant cavity (Q_{int}) using the formula [21]

$$Q_{\text{int}} = \frac{2Q_{\text{load}}}{1 + \sqrt{T_0}}, \qquad (2)$$

where T_0 s the fraction of optical power exiting the ring resonant cavity at the resonance wavelength λ_0.

The intrinsic quality factor value and known material characteristics enable calculation of the optical loss magnitude α (Fig. 4, *c*) in the ring resonant cavity:

$$\alpha = \frac{2\pi n_g}{Q_{\text{int}}\lambda_0}, \qquad (3)$$

where n_g is the group refractive index.

Discussion of findings

Analysis of spectral characteristics (Fig. 3) and determination of ring resonator parameters revealed that low-temperature Si$_3$N$_4$ deposition by LPCVD at 350 °C failed to yield layers with optical properties suitable for fabricating waveguide elements. The best results in this work were achieved with structures featuring microring resonant cavities fabricated using high-temperature (750 °C) Si$_3$N$_4$.

At the next stage, substrates with high-temperature amorphous Si$_3$N$_4$ that underwent additional annealing at 1200 °C in an N$_2$ atmosphere were investigated. Annealing was performed to remove residual hydrogen from Si$_3$N$_4$ films by breaking N-H bonds. The impact of annealing on layer characteristics was assessed via FTIR spectroscopy on a „Bruker VERTEX 70v“ instrument (Fig. 4), which confirmed reduced H$_2$ content in the amorphous Si$_3$N$_4$

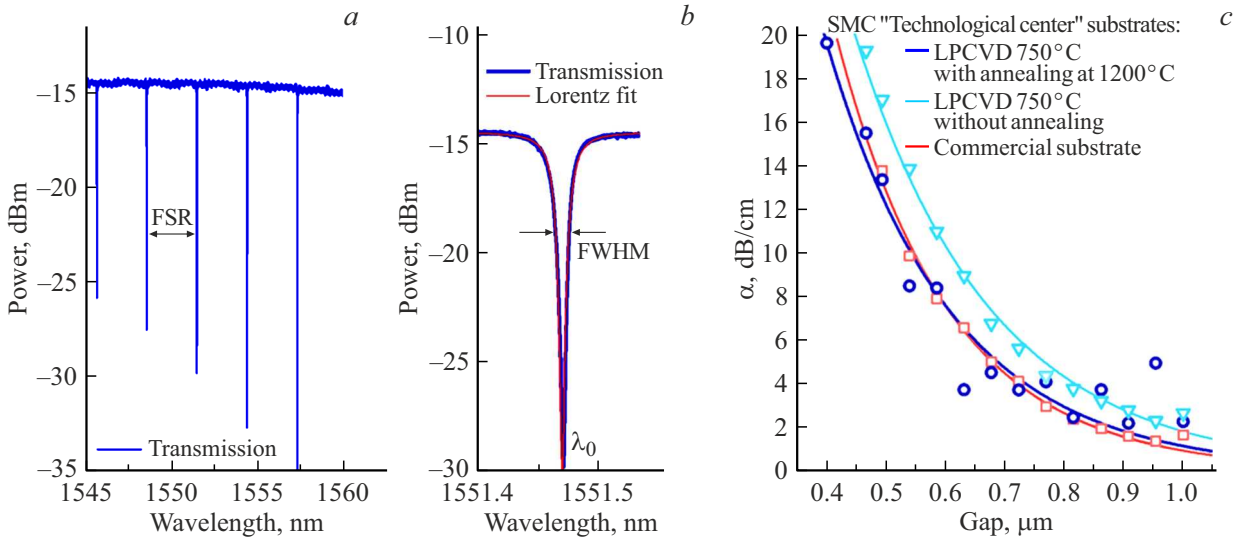

Figure 5. Spectral characteristic of a ring resonant cavity (a), single resonance with $Q_{int} \approx 3 \cdot 10^5$ and its approximation (b), comparison of optical losses for samples fabricated using different substrates (c).

layer. Differences in spectra from unannealed and annealed wafers were also observed, attributable to lowered hydrogen content in the silicon nitride layer, consistent with findings from other published studies [22,23].

Analysis of transmission spectra from fabricated waveguide structures showed that nitrogen-atmosphere annealing positively affects formed structure parameters, particularly optical losses (Fig. 5, c) and diffraction grating efficiency (Fig. 3). Annealing had no effect on the FSR parameter of fabricated structures, which was 2.9 nm across all samples. FSR.

Comparison of microcavity characteristics fabricated on substrates from the SIC„Technology center“ with those on a commercial foreign substrate of identical geometry demonstrated comparable parameters, including optical losses (Fig. 5, c) but superior coupling efficiency for structures based on SIC „Technology center“, substrates, as evidenced by the spectral envelope positions in Fig. 3.

Notably, this work did not achieve record Q values for ring resonators (per formulas (1) and (2), maxima reached $Q_{int} = 3 \cdot 10^5$) compared to prior publications [24–33]. Nevertheless, the developed technology for $SiO_2$and Si_3N_4 layer formation on 100 mm silicon monocrystalline substrates enables reproducible fabrication of high-Q resonant cavities under production conditions. The table lists approaches used in literature to enhance ring resonant cavity parameters, including Q values. For the developed technology, further improvements may arise from etching process and geometry optimization.

Conclusion

Thus, optimal results were obtained using high-temperature amorphous Si_3N_4 layer deposition by LPCVD followed by annealing. Microring resonant cavities formed on these substrates exhibited $Q_{int} \approx 3 \cdot 10^5$ and $FSR \approx 2.9$ nm.

Methods for reducing losses in microring resonant cavities

Loss reduction method	Achieved Q value
Optical mode delocalization	$8 \cdot 10^7$ [23]
	$2.6 \cdot 10^8$ [24]
Surface roughness reduction	$3.7 \cdot 10^7$ [25]
Multi-stage waveguide annealing	$8.5 \cdot 10^6$ [26]
Damascene process with (reflow) SiO_2	$5 \cdot 10^6$ [27]
Microring cavity geometry optimization	$3.2 \cdot 10^7$ [28]
Hybrid scheme	$2 \cdot 10^7$ [29]
Fabrication process optimization	$1.1 \cdot 10^7$ [30]
Elimination of Si_3N_4film cracks due to internal stresses	$1.5 \cdot 10^6$ (TM mode) [31]
Microcavity	$4.57 \cdot 10^7$ geometry optimization [32]

In this paper, a number of basic technological operations are presented for the sequential formation of SiO_2 and Si_3N_4 layers with thicknesses of 2.7 and 0.45 μm respectively, on the surface of 100 mm silicon single-crystal substrates. Using these layers, photonic integrated circuits (PICs) with thin-film waveguides, input/output elements, and high-Q ring microcavities were made.

Transmission spectrum studies established experimental dependencies of ring resonator parameters on structure formation regimes and resonant cavity geometry. Microring resonant cavities made with optimal SiO_2 and Si_3N_4 layer regimes demonstrate 10^5. Elements made on SIC „Technology center“ substrates are nearly comparable to commercial

foreign analogs. Further enhancements, including loss reduction, may be achieved via etching and geometry optimization.

Funding

Technology development, functional layer formation, and ring resonator fabrication were supported by Russian Science Foundation grant № 23-91-06308 (https://rscf.ru/project/23-91-06308/). Photonic structure simulation and design were funded by the Ministry of Science and Higher Education of the Russian Federation (FNRM-2025-0014).

Conflict of interest

The authors declare that they have no conflict of interest.

References

[1] J. Capmany et al. Nat. Phot., **1** (6), 319 (2007). DOI: 10.1038/nphoton.2007.89
[2] Y. Jiao. Master Thesis Work (Polytechnic University of Catalonia (UPC), B., (2015). URL: https://upcommons.upc.edu/entities/publication/37edf1c3-5098-4550-b081-07785d69cf98
[3] R.C. Williamson, R.D. Esman. J. Lightw. Technol., **26** (9), 1145 (2008). DOI: 10.1109/JLT.2008.923627
[4] J.P. Yao. J. Lightw. Technol., **27** (3), 314 (2009). DOI: 10.1109/JLT.2008.2009551
[5] K.A. Williams, E.A.J.M. Bente, D. Heiss, Y. Jiao, K. Ławniczuk, X.J.M. Leijtens, J.J.G.M. van der Tol, M.K. Smit. Photon. Res., **3** (5), B60 (2015). DOI: 10.1364/PRJ.3.000B60
[6] M. Smit et al. Semiconductor Science and Technol., **29** (083001), 1 (2014). DOI: 10.1088/0268-1242/29/8/08300
[7] J. Liu, A.S. Raja, M. Karpov, B. Ghadiani, M.H.P. Pfeiffer, B. Du, N.J. Engelsen, H. Guo, M. Zervas, T.J. Kippenberg. Opt., **5** (10), 1347 (2018). DOI: 10.1364/OPTICA.5.001347
[8] Y.Z. Twayana, K. Andrekson, V.T. Company. Opt. Express, **27** (24), 35719 (2019). DOI: 10.1364/OE.27.035719
[9] H.E. Dirani, L. Youssef, C. Petit-Etienne, S. Kerdiles, P. Grosse, C. Monat, E. Pargon, C. Sciancalepore. Opt. Express, **27** (21), 30726 (2019). DOI: 10.1364/OE.27.030726
[10] Q. Li, M. Davanco, K. Srinivasan. Nat. Photonics, **10**, 406 (2016). DOI: 10.1038/nphoton.2016.64
[11] X. Lu, G. Moille, Q. Li et al. Nat. Photonics, **13** (9), 593 (2019). DOI: 10.1038/s41566-019-0464-9
[12] Y. Xuan et al. Opt., **3** (11), 1171 (2016). DOI: 10.1364/OPTICA.3.001171
[13] X. Ji et al. Opt., **4** (6), 619 (2017). DOI: 10.1364/OPTICA.4.000619
[14] I.V. Ivashenceva, I.V. Tret'yakov, N.S. Kaurova, A.D. Golikov, G.N. Gol'cman. Opt. i spektr., **132** (10), 1076–1086 (2024) (in Russian). DOI: 10.61011/OS.2024.10.59423.7024-24
[15] S. Xiao, M.H. Khan, H. Shen, M. Qi. J. Lightw. Technol., **26** (2), 228 (2008). DOI: 10.1109/JLT.2007.911098
[16] A. Densmore, D. Xu, P. Waldron, S. Janz, P. Cheben, J. Lapointe, A. Delâge, B. Lamontagne, J.H. Schmid, E. Post. IEEE Phot. Technol. Lett., **18** (23), 2520 (2006). DOI: 10.1109/LPT.2006.887374
[17] S.K. Selvaraja, P. Jaenen, W. Bogaerts, D. van Thourhout, P. Dumon, R. Baets. J. Lightw. Technol., **27** (18), 4076 (2009). DOI: 10.1109/JLT.2009.2022282
[18] A. Nikitin, A. Ustinov. ZhTF, **94** (8), 1382–1390 (2024) (in Russian). DOI: 10.61011/JTF.2024.08.58567.72-24
[19] V.A. Kiselevskij, K.A. Fetisenkova, A.A. Tatarincev, A.E. Mel'nikov, O.G. Glaz. Opt. i spektr., **133** (3), 292–298 (2025) (in Russian). DOI: 10.61011/OS.2025.03.60246.2-25
[20] S.S. Kosolobov, I.A. Pshenichnyuk, K.R Taziev, A.K. Zemtsova, D.S. Zemtsov, A.S. Smirnov, D.M. Zhigunov, V.P. Drachev. UFN, **194** (in Russian). 1223–1239 (2024). DOI: 10.3367/UFNr.2024.09.039762
[21] P. An et al. Journal of Physics: Conference Series, **1124**, 51047 (2018). DOI: 10.1088/1742-6596/1124/5/051047
[22] H. El Dirani, L. Youssef, C. Petit-Etienne et al. Opt. Express, **27**, 30726–30740 (2019). DOI: 10.1364/OE.27.030726
[23] A. Chhoker et al. ChemistrySelect, **10** (2025). DOI: 10.1002/slct.202404474
[24] D.T. Spencer, J.F. Bauters, M.J.R. Heck, J.E. Bowers. Optica, **1**, 153 (2014). DOI: 10.1364/OPTICA.1.000153
[25] W. Jin, Q.-F. Yang, L. Chang, B. Shen, H. Wang, M.A. Leal, L. Wu, M. Gao, A. Feshali, M. Paniccia, K.J. Vahala, J.E. Bowers. Nat. Photonics, **15**, 346–353 (2021). DOI: 10.1038/s41566-021-00761-7
[26] X. Ji, F.A.S. Barbosa, S.P. Roberts, A. Dutt, J. Cardenas, Y. Okawachi, A. Bryant, A.L. Gaeta, M. Lipson. Optica, **4**, 619–624 (2017). DOI: 10.1364/OPTICA.4.000619
[27] H.El. Dirani, L. Youssef, C. Petit-Etienne, S. Kerdiles, P. Grosse, C. Monat, E. Pargon, C. Sciancalepore. Opt. Express, **27**, 30726–30740 (2019). DOI: 10.1364/OE.27.030726
[28] M.H.P. Pfeiffer, J. Liu, A.S. Raja, T. Morais, B. Ghadiani, T.J. Kippenberg. Optica, **5**, 884 (2018). DOI: 10.1364/OPTICA.5.000884
[29] X. Ji, J.K. Jang, U.D. Dave, M. Corato-Zanarella, C. Joshi, A.L. Gaeta, M. Lipson. Laser Photonics Rev., **15**, 2000353 (2021). DOI: 10.48550/arXiv.2012.04191
[30] Li Q et al. Opt. Express, **21**, 18236–18248 (2013). DOI: 10.1364/OE.21.018236
[31] Zhichao Ye, et al. Opt. Express, **27**, 35719–35727 (2019). DOI: 10.48550/arXiv.1909.10251
[32] Shuai Wan, Rui Niu, Jin-Lan Peng, Jin Li, Guang-Can Guo, Chang-Ling Zou, Chun-Hua Dong. Chin. Opt. Lett., **20**, 032201 (2022). DOI: 10.3788/COL202220.032201
[33] S. Cui et al. arXiv:2209.01097 (2022). DOI: 10.48550/arXiv.2209.01097

Translated by J.Savelyeva